Design of Laminated Plates for Maximum Buckling Load

Yung S. Sing, Raphael T. Haftka,
Layne T. Watson and Raymond H. Plaut

TR 88-14

DESIGN OF LAMINATED PLATES FOR MAXIMUM BUCKLING LOAD

Yung S. Shin*, Raphael T. Haftka**, Layne T. Watson†, and Raymond H. Plaut‡

Virginia Polytechnic Institute and State University
Blacksburg, VA 24061

ABSTRACT

The buckling load of laminated plates having midplane symmetry is maximized for a given total thickness. The thicknesses of the layers are taken as the design variables. Buckling analysis is carried out using the finite element method. The optimality equations are solved by a homotopy method which permits tracing optima as a function of total thickness. It is shown that for any design with a given stacking sequence of ply orientations, there exists a design associated with any other stacking sequence which possesses the same bending stiffness matrix and same total thickness. Hence, from the optimum design for a given stacking sequence, one can directly determine the optimum design for any rearrangement of the ply orientations, and the optimum buckling load is independent of the stacking sequence.

* Graduate Student, Department of Civil Engineering

** Professor, Department of Aerospace and Ocean Engineering, Member AIAA

† Professor, Department of Computer Science

‡ Professor, Department of Civil Engineering, Member ASME

1. Introduction

Composite materials are ideal for structural applications where high strength-to-weight and stiffness-to-weight ratios are required. Design optimization of composite structures has gained importance in recent years as the engineering applications of fiber-reinforced materials have increased and weight savings has become an essential design objective, especially for aircraft and spacecraft structures.

Previous work on the optimal design of composite plates has focused on optimization with respect to the fiber orientations [1-10]. In Refs. [11-16], however, laminate optimization is considered, in which the thicknesses of plies with specified orientation angles are treated as the design variables. The thickness of material at each preassigned orientation is treated as a continuous variable. More sophisticated approaches dealing with discrete values for the thicknesses by employing integer variables are presented by Mesquita and Kamat [17, 18] and Olson and Vanderplaats [19]. The present paper avoids the difficulties associated with discrete or integer variables by treating the thickness variables as continuous variables.

A recently developed design method for buckling load maximization [20] starts from a given optimum design point and traces optimum designs as a function of the amount of available material. The method employs a homotopy technique [21] that has been widely used in many fields of engineering. In Ref. [20], the method was formulated using a simultaneous analysis and design approach and applied to the design of columns on elastic foundations. One objective of the present paper is to apply the same method with the more traditional nested approach in which the buckling analysis is performed repeatedly. A second objective is to study the effect of the stacking sequence on the optimum design. For this second objective we start by proving a useful result on the equivalence of plates with different stacking sequences.

2. Bending stiffness matrix invariance to changes in stacking sequence

The laminates considered in this study are symmetric about the middle surface, so that the bending response is not coupled to the membrane action. The moment-curvature relations are then expressed in the form

$$\{M\} = \begin{Bmatrix} M_X \\ M_Y \\ M_{XY} \end{Bmatrix} = \begin{bmatrix} D_{11} & D_{12} & D_{16} \\ D_{12} & D_{22} & D_{26} \\ D_{16} & D_{26} & D_{66} \end{bmatrix} \begin{Bmatrix} \kappa_X \\ \kappa_Y \\ \kappa_{XY} \end{Bmatrix} = [D]\{\kappa\}, \tag{1}$$

where [D] is the laminate bending stiffness matrix, {M} is the bending and twisting moments per unit length, and $\{\kappa\}$ is the corresponding curvatures given by

$$\begin{Bmatrix} \kappa_X \\ \kappa_Y \\ \kappa_{XY} \end{Bmatrix} = \left\{ -\frac{\partial^2 W}{\partial X^2} \quad -\frac{\partial^2 W}{\partial Y^2} \quad -2\frac{\partial^2 W}{\partial X \partial Y} \right\}^T. \tag{2}$$

Figure 1 shows the geometry of a laminate with 2n layers. The Z axis is taken perpendicular to the midplane of the laminate and is positive in the downward direction. Below the midplane, the value of Z at the bottom of layer k is denoted Z_k. The thicknesses of the layers are given by

$$T_i = Z_i - Z_{i+1}, \qquad \text{for } i = 1, 2, \ldots, n, \tag{3}$$

with $Z_{n+1} = 0$.

Using classical lamination theory, the bending stiffness matrix [D] in Eq. (1) can be written as

$$[D] = \frac{2}{3}\sum_{k=1}^{n} [\bar{Q}]_k (Z_k^3 - Z_{k+1}^3), \tag{4}$$

where $[\bar{Q}]_k$ is the transformed reduced stiffness matrix of the k-th layer, which can be defined in terms of the ply angle ϕ and elastic constants E_{11}, E_{22}, ν_{12} and G_{12} of the orthotropic layer as

$$[\bar{Q}]_k = [T]_k^{-1}[Q][T]_k^{-T}. \tag{5}$$

The superscript -1 denotes the matrix inverse and -T denotes the transpose of the inverse matrix. The matrix $[T]_k$ is the coordinate transformation matrix and [Q] is the reduced stiffness matrix, given by

$$[T]_k = \begin{bmatrix} \cos^2\phi_k & \sin^2\phi_k & \sin 2\phi_k \\ \sin^2\phi_k & \cos^2\phi_k & -\sin 2\phi_k \\ -\sin\phi_k\cos\phi_k & \sin\phi_k\cos\phi_k & \cos 2\phi_k \end{bmatrix},$$

$$[Q] = \begin{bmatrix} E_{11}/(1-\nu_{12}\nu_{21}) & \nu_{12}E_{22}/(1-\nu_{12}\nu_{21}) & 0 \\ \nu_{12}E_{22}/(1-\nu_{12}\nu_{21}) & E_{22}/(1-\nu_{12}\nu_{21}) & 0 \\ 0 & 0 & G_{12} \end{bmatrix}. \tag{6}$$

The bending stiffness matrix will now be shown to have an important property: when the stacking sequence is changed, we can always recover the original bending stiffness matrix by appropriately changing layer thicknesses while preserving the total laminate thickness. This property is proved in two steps. First, it is shown that when the ply orientations in two adjacent layers are interchanged, there exists an equivalent design with the same bending stiffness and the same total thickness. Then we show by induction that the same property applies to the general rearrangement of all layers.

Consider a symmetric laminated plate with 2n layers (Fig. 2-a). The elements of the original bending stiffness matrix are given by

$$D_{ij}^a = \frac{2}{3}\sum_{k=1}^{\tau-2}(\bar{Q}_{ij})_k(Z_k^3 - Z_{k+1}^3) + \frac{2}{3}(\bar{Q}_{ij})_{\tau-1}(Z_{\tau-1}^3 - Z_\tau^3) + \frac{2}{3}(\bar{Q}_{ij})_\tau(Z_\tau^3 - Z_{\tau+1}^3)$$
$$+ \frac{2}{3}\sum_{k=\tau+1}^{n}(\bar{Q}_{ij})_k(Z_k^3 - Z_{k+1}^3) \qquad \text{for i, j = 1, 2, 6.} \tag{7}$$

When the ply orientations in the $\tau-1$ and τ layers are interchanged (shown in Fig. 2-b), we can still obtain the same D_{ij} by changing the thicknesses of layers $\tau-1$ and τ. The bending stiffness of the laminate in Fig. 2-b is

$$D_{ij}^{b} = \frac{2}{3}\sum_{k=1}^{\tau-2}(\overline{Q}_{ij})_k(Z_k^3 - Z_{k+1}^3) + \frac{2}{3}(\overline{Q}_{ij})_\tau(Z_{\tau-1}^3 - Z_*^3) + \frac{2}{3}(\overline{Q}_{ij})_{\tau-1}(Z_*^3 - Z_{\tau+1}^3)$$
$$+ \frac{2}{3}\sum_{k=\tau+1}^{n}(\overline{Q}_{ij})_k(Z_k^3 - Z_{k+1}^3) \qquad \text{for i, j = 1, 2, 6.} \tag{8}$$

where Z_* is the new height of the bottom of layer τ, determined so that the two plates have the same bending stiffness. Setting $D_{ij}^a = D_{ij}^b$ from Eqs. (7) and (8), we obtain

$$\{(\overline{Q}_{ij})_\tau - (\overline{Q}_{ij})_{\tau-1}\}\{Z_*^3 - Z_{\tau-1}^3 + Z_\tau^3 - Z_{\tau+1}^3\} = 0 \qquad \text{for i, j = 1, 2, 6.} \tag{9}$$

These equations are satisfied for arbitrary $\overline{Q}$'s if Z_* is chosen such that

$$Z_* = \sqrt[3]{Z_{\tau-1}^3 - Z_\tau^3 + Z_{\tau+1}^3}\,. \tag{10}$$

Since $Z_{\tau-1} \geq Z_\tau \geq Z_{\tau+1}$, $Z_{\tau+1}^3 - Z_\tau^3 \leq 0$ and, from Eq. (10), $Z_* \leq Z_{\tau-1}$. Similarly, $Z_{\tau-1}^3 - Z_\tau^3 \geq 0$ so that $Z_* \geq Z_{\tau+1}$. Hence the height Z_* always falls between $Z_{\tau-1}$ and $Z_{\tau+1}$. This shows that there always exists a design producing the same bending stiffness matrix [D] when ply orientations in two adjacent layers are interchanged.

The general results for interchanging ply orientations in any number of layers follows by induction, because a general interchange is a sequence of transpositions. For example, an equivalent design for a $(45°/90°/0°)_s$ laminate can be obtained from a $(0°/90°/45°)_s$ laminate using three transpositions and thicknesses recomputed by Eq. (10). First, we obtain an equivalent design for a $(90°/0°/45°)_s$ laminate from the $(0°/90°/45°)_s$ laminate, then a $(90°/45°/0°)_s$ laminate is obtained from the $(90°/0°/45°)_s$ laminate, and finally the $(45°/90°/0°)_s$ laminate is obtained from the $(90°/45°/0°)_s$.

It should be noted that the above transformation changes the individual thicknesses of the original laminate. Therefore the membrane stiffness is changed, while the bending stiffness remains the same. The existence of multiple laminate designs with the same total thickness and the same

bending stiffness has important implications for the optimization process in that it results in multiple optima, as will be shown in the examples in Section 5.

3. Buckling analysis

The plate we consider is simply supported along all four edges and subject to uniform in-plane loading in the X-direction, as shown in Fig. 3. The dimensions of the plate in the X and Y directions are a and b, respectively. Half the thickness of the plate is denoted by T_T and is considered small in comparison with the other dimensions. Shear deformation is not considered in the analysis.

The differential equation for the buckling analysis is given by

$$\frac{\partial^2 M_X}{\partial X^2} + 2\frac{\partial^2 M_{XY}}{\partial X \partial Y} + \frac{\partial^2 M_Y}{\partial Y^2} - N_X \frac{\partial^2 W}{\partial X^2} = 0, \tag{11}$$

where N_X is the buckling load and W denotes the transverse deflection of the middle surface of the plate. The moments are given in Eq. (1).

The analysis is performed with dimensionless quantities. First, using the nondimensional material properties,

$$e_{22} = \frac{E_{22}}{E_{11}}, \qquad g_{12} = \frac{G_{12}}{E_{11}}, \tag{12}$$

the nondimensional reduced stiffness matrix is

$$[\bar{q}]_k = \frac{1}{E_{11}}[\bar{Q}]_k = [T]_k^{-1} \begin{bmatrix} 1/(1-\nu_{12}\nu_{21}) & \nu_{12}e_{22}/(1-\nu_{12}\nu_{21}) & 0 \\ \nu_{12}e_{22}/(1-\nu_{12}\nu_{21}) & e_{22}/(1-\nu_{12}\nu_{21}) & 0 \\ 0 & 0 & g_{12} \end{bmatrix} [T]_k^{-T}. \tag{13}$$

Quantities relating to plate thickness such as Z_i, T_T, and T_i are normalized by T_{Tmax}, the maximum total thickness considered in the optimization study:

$$z_i = \frac{Z_i}{T_{Tmax}}, \qquad t_T = \frac{T_T}{T_{Tmax}}, \qquad t_i = \frac{T_i}{T_{Tmax}}. \tag{14}$$

Substituting Eqs. (13) and (14) into Eq. (4), we obtain the nondimensional laminate stiffness matrix

$$[d] = \frac{1}{E_{11} T_{Tmax}^3} [D] = \frac{2}{3} \sum_{k=1}^{n} [\overline{q}]_k (z_k^3 - z_{k+1}^3). \tag{15}$$

The coordinates and displacements are nondimensionalized by the plate length in the x-direction, a:

$$x = \frac{X}{a}, \qquad y = \frac{Y}{a}, \qquad w = \frac{W}{a}, \tag{16}$$

and the nondimensional moments, m_x, m_y, and m_{xy} are defined as

$$\begin{Bmatrix} m_x \\ m_y \\ m_{xy} \end{Bmatrix} = \frac{a}{E_{11} T_{Tmax}^3} \begin{Bmatrix} M_X \\ M_Y \\ M_{XY} \end{Bmatrix} = [d] \begin{Bmatrix} -\frac{\partial^2 w}{\partial x^2} & -\frac{\partial^2 w}{\partial y^2} & -2\frac{\partial^2 w}{\partial x \partial y} \end{Bmatrix}^T. \tag{17}$$

Finally, using Eqs. (16) and (17) the original buckling differential equation is transformed to

$$\frac{\partial^2 m_x}{\partial x^2} + 2\frac{\partial^2 m_{xy}}{\partial x \partial y} + \frac{\partial^2 m_y}{\partial y^2} - n_x \frac{\partial^2 w}{\partial x^2} = 0, \tag{18}$$

where n_x is the nondimensional buckling load defined by

$$n_x = \frac{a^2}{E_{11} T_{Tmax}^3} N_X. \tag{19}$$

The differential equation is solved by the finite element method using a 16-degree-of-freedom element first introduced by Bogner, Fox, and Schmit [23].

Assuming the in-plane load is uniform, the finite element discretization of Eq. (18) is

$$[K]\{U\} - n_x[K_G]\{U\} = 0, \tag{20}$$

where [K] is the system stiffness matrix, $[K_G]$ is the system geometric stiffness matrix, and {U} is the buckling mode. The above matrix equation is solved using SNLASO, one of the subroutines from the package LASO2 [24], which computes a few eigenvalues and the associated eigenvectors of a large (sparse) symmetric matrix using the Lanczos algorithm [25].

The optimization procedure requires derivatives of the buckling load with respect to the thickness variables t_i. These are calculated explicitly by differentiating the Rayleigh quotient associated with Eq. (20):

$$\frac{dn_x}{dt_i} = \frac{\{U\}^T \frac{\partial[K]}{\partial t_i}\{U\}}{\{U\}^T[K_G]\{U\}}. \tag{21}$$

The stiffness matrix derivatives are estimated by forward finite difference approximations.

Sometimes the optimum design is bimodal, in which case there are two eigenvectors corresponding to the lowest eigenvalue. The buckling load is not differentiable for this case. To eliminate this difficulty, we use a constraint, $n_{x1} = 0.999\, n_{x2}$ in the bimodal formulation (see Appendix) so that the buckling modes can be determined separately for the first buckling load, n_{x1} , and the second buckling load, n_{x2} .

4. Optimization method

The optimization problem that we consider here is to maximize the buckling load of a plate for a given total plate thickness. The thickness of each layer is assumed to be constant over the plate, and for a given stacking sequence of the layers, each thickness is taken as a design variable. The nondimensional thicknesses, t_i, are subject to bound constraints

$$t_{min} \le t_i \le t_{max} \qquad \text{for } i = 1, \ldots, n, \tag{22}$$

where t_{max} and t_{min} are upper and lower bounds, respectively.

The optimization problem is written as

$$\max_{t_i} \quad n_x \tag{23}$$

$$\text{such that} \quad \sum_{i=1}^{n} t_i - t_T = 0$$

$$\text{and} \quad t_{min} \le t_i \le t_{max} \qquad \text{for } i = 1, \ldots, n,$$

where the nondimensional buckling load, n_x, is obtained by solving Eq. (20).

A typical optimization method, applied to solve this problem, starts from a given design and continuously searches for better designs until it finds one optimum design. The intermediate designs along the path are of no interest to the structural designer. Here, instead, we use a method which traces an entire one-parameter family of optimal designs without going through any intermediate nonoptimal designs. For this we employ the homotopy method, a technique which has been used widely to solve nonlinear systems of equations. The basic idea of the method is to convert the system of equations into a set of ordinary differential equations with a parameter, called a homotopy parameter. Under certain assumptions, the method is guaranteed to converge to a solution even for highly nonlinear problems for which Newton-type iteration methods fail. The total thickness of the plate, t_T , is chosen as the homotopy parameter, and for the initial conditions for the initial value problem we use the minimum-thickness plate with t_T corresponding to all design variables at their lower bound. The trajectory of the initial value problem is a path of optima corresponding to varying t_T. The independent variable for the ordinary differential equation is arc length along this trajectory. This use of the homotopy method for tracing optima was suggested in [20] with a simultaneous analysis and design formulation for a column with a variable elastic foundation. Here the method is used with the traditional nested formulation in which the buckling loads are computed in a separate analysis.

The equations defining the path of optimal designs are obtained using Lagrange multipliers, and are solved by the homotopy method as described in [21]. The optimum path consists of several smooth segments, with breaks in smoothness at points where the active constraint set changes. Changes in active constraints are associated with inequality constraints (here bound constraints on design variables) which may become active or inactive along the path. Along each segment, the active inequality constraints are treated as equality constraints,

$$t_j = t_{min} \quad \text{or} \quad t_j = t_{max} \qquad \text{for } j \in I_A, \tag{24}$$

where I_A is the set of indices of thicknesses which are at a lower or upper bound. These variables are eliminated from the optimization problem, while the other variables are left unconstrained. The optimization problem along a segment can, therefore, be written as

$$\max_{t_i} \quad n_x \qquad \text{for } i \notin I_A \tag{25}$$

$$\text{such that} \quad \sum_{i=1}^{n} t_i - t_T = 0. \tag{26}$$

The solution of the above problem requires dealing with three related problems: solving the optimization problem along a segment, locating the end of the segment where the set I_A changes, and finding the set I_A for the next segment.

4.1 Stationary conditions

Using a Lagrange multiplier μ, the augmented function n_x^* is

$$n_x^* = n_x - \mu[\sum_{i=1}^{n} t_i - t_T]. \tag{27}$$

Taking the first derivatives of n_x^* with respect to t_i and μ, and setting them equal to zero, we obtain the optimality conditions

$$\frac{\partial n_x}{\partial t_i} - \mu = 0 \qquad \text{for } i \notin I_A \tag{28}$$

and the total thickness constraint of Eq. (26). Equations (26) and (28) form a system of nonlinear equations to be solved for t_i and μ. A homotopy method is used to find the solution of these equations for varying t_T.

In certain ranges of structural resources, the optimal solution may be bimodal, i.e., the lowest buckling load may be a repeated eigenvalue. The formulation for bimodal solutions is given in the Appendix. The existence of bimodal solutions also introduces additional transitions (bimodal to unimodal and vice versa) along the path of optimum solutions.

4.2 Locating transition points

There are four types of events which end a segment and start a new one:

Type 1: A bound constraint becoming active (i.e., being satisfied as an equality);

Type 2: A bound constraint becoming inactive;

Type 3: Transition from a unimodal solution to a bimodal solution;

Type 4: Transition from a bimodal solution to a unimodal solution.

Transition points of type 1 are located by checking the bound constraints (22).

Transition points of type 2 are checked by using the Kuhn-Tucker conditions. The solution satisfies the Kuhn-Tucker conditions when all Lagrange multipliers are nonnegative, so a transition of type 2 is detected by a Lagrange multiplier associated with a bound constraint becoming negative. These multipliers are obtained by replacing the augmented function n_x^* (for the unimodal case) in Eq. (27) by

$$n_x^* = n_x - \mu[\sum_{i=1}^{n} t_i - t_T] - \sum_{i \in I_A} \lambda_{1i}[t_{min} - t_i] - \sum_{i \in I_A} \lambda_{2i}[t_i - t_{max}]. \tag{29}$$

Taking the first derivatives of n_x^* with respect to t_i and setting them equal to zero, we obtain

$$\frac{\partial n_x}{\partial t_i} - \mu + \lambda_{1i} - \lambda_{2i} = 0 \qquad \text{for } i \in I_A. \tag{30}$$

Since $\lambda_{1i} = 0$ for $t = t_{max}$ and $\lambda_{2i} = 0$ for $t = t_{min}$, λ_{1i} and λ_{2i} are given by

$$\begin{aligned} \lambda_{1i} &= -\frac{\partial n_x}{\partial t_i} + \mu \qquad \text{for } t_i = t_{min} \\ \lambda_{2i} &= \frac{\partial n_x}{\partial t_i} - \mu \qquad \text{for } t_i = t_{max}. \end{aligned} \tag{31}$$

Similar equations for the bimodal case are given in the Appendix.

A transition of type 3 occurs when two buckling loads approach together and meet, as shown in Fig. 4. Previous works [20, 26] indicate that the optimal design may remain bimodal for the subsequent segment on the solution path. The homotopy routine traces solutions on a smooth path using sensitivity information obtained from the previous point. To preserve the smoothness of the solution path, the tracing routine picks at each step the eigenvalue n_x corresponding to the critical n_x in the previous step. As soon as the transition is passed this n_x is no longer the lowest one, and this event identifies transition type 3.

The bimodal formulation includes an additional constraint for the bimodality requirement (see Appendix), and this constraint is handled with a Lagrange multiplier γ. The following inequality is necessary in the bimodal range and can be used to detect the type 4 transition from bimodal to unimodal:

$$0 \le \gamma \le 1. \tag{32}$$

4.3 Choosing an optimum path

At a transition point there are a number of solution paths which satisfy the stationary equations, so we need to choose a path which satisfies the optimality conditions. Choosing an optimum path constitutes finding a set of active bound constraints for type 1 and 2 transitions and the correct buckling modes for type 3 and 4 transitions. These are obtained by using the Lagrange multipliers of the previous path and the buckling load derivatives. The procedure is explained separately for each type of transition.

A type 1 transition occurs when one of design variables, t_i , reaches its upper or lower bound. Then t_i is set to t_{max} or t_{min} and treated as a constant value. The number of design variables is reduced by one.

At a type 2 transition, one of the Lagrange multipliers for the bound constraints, λ_{1i} or λ_{2i}, is found to be negative. The bound constraint corresponding to the negative λ_{1i} or λ_{2i} is set to be inactive and the number of design variables is increased by one.

At a transition from a unimodal solution to a bimodal solution (a type 3 transition), the bimodal stationary conditions given in the Appendix replace the unimodal stationary conditions (Eqs. (26) and (28)).

At a transition from a bimodal to a unimodal solution (a type 4 transition), two buckling modes are given from the bimodal solution, and only one has to be chosen for the forthcoming unimodal solution path. The Lagrange multiplier for the bimodality constraint, γ, is checked with respect to the inequality (32) at the previous transition point. When γ is larger than 1, the mode corresponding to n_{x2} is chosen, and when γ is smaller than 0, the mode corresponding to n_{x1} is chosen.

Some of the above transitions can occur simultaneously. Special treatment is required in certain cases where the Lagrange multipliers are not available. In general, the optimum design requires at least one design variable t_i for a unimodal case and two design variables for a bimodal case. At a

type 1 transition, the number of design variables is reduced by one, and at a type 3 transition the bimodal formulation requires one more design variable in case the previous unimodal path has only one design variable. Therefore some type 1 or type 3 transitions occur simultaneously with a type 2 transition which allows an additional design variable. In that case, the Lagrange multipliers λ_{1i} and λ_{2i}, which are used at a type 2 transition to determine a new design variable, are not available. We then rely on the derivative of n_x with respect to t. For a unimodal case, the location of the new design variable t_i is determined where dn_x/dt_T is maximized. For a bimodal case, we need to find a combination of t_i and t_j which maximizes the value of the dn_x/dt_T. Considering the bound constraints in the formulation, the new design variables are determined by

$$\max_{i,\,j} \quad \frac{dn_{x1}}{dt_T} = \frac{\partial n_{x1}}{\partial t_i}\frac{dt_i}{dt_T} + \frac{\partial n_{x1}}{\partial t_j}\frac{dt_j}{dt_T} \tag{33}$$

$$\text{such that} \quad \frac{\partial n_{x1}}{\partial t_i}\frac{dt_i}{dt_T} + \frac{\partial n_{x1}}{\partial t_j}\frac{dt_j}{dt_T} = \frac{\partial n_{x2}}{\partial t_i}\frac{dt_i}{dt_T} + \frac{\partial n_{x2}}{\partial t_j}\frac{dt_j}{dt_T}$$

$$\frac{dt_i}{dt_T} \geq 0 \quad \text{for} \quad t_i = t_{min}$$

$$\frac{dt_i}{dt_T} \leq 0 \quad \text{for} \quad t_i = t_{max}$$

$$\frac{dt_j}{dt_T} \geq 0 \quad \text{for} \quad t_j = t_{min}$$

$$\text{and} \quad \frac{dt_j}{dt_T} \leq 0 \quad \text{for} \quad t_j = t_{max}$$

where n_{x1} and n_{x2} are the first and the second buckling load, respectively.

After we obtain the design variables t_i, we need the Lagrange multipliers μ and γ at the transition point to complete the set of starting values for the next solution path. These are obtained by solving the stationary conditions for the given t_i. For example, in the unimodal case, μ is obtained by solving one of the optimality conditions (28).

5. Results

Some examples are presented to demonstrate the effect of optimization of layer thicknesses on the buckling of laminated plates. A graphite/epoxy composite plate is selected and its material properties are given by $E_{11} = 31.0\text{x}10^6$ psi, $E_{22} = 3.4\text{x}10^6$ psi, $G_{12} = 0.75\text{x}10^6$ psi, and $\nu_{12} = 0.28$, corresponding to nondimensional properties $e_{22} = 0.1097$, $g_{12} = 0.02419$. The plate aspect ratio (a/b) is chosen to be 1.2.

To determine an appropriate mesh size for the finite element analysis, a series of numerical tests were performed for a $(0°/90°/45°)_s$ laminate. The nondimensional thickness of each layer was set at 1/3. Table 1 shows the first and second buckling loads for different meshes. The first buckling load is quite accurate even for a 2x2 mesh (less than 1 % difference compared to the 6x6 mesh); however, the second buckling load, which has a full sine mode in the x-direction, converges more slowly as the mesh is refined. Since the optimum designs are often bimodal, the first two buckling loads must be considered in the analysis, and a 4x4 mesh is chosen for the finite element analysis.

First, optimization results are presented for this $(0°/90°/45°)_s$ laminate for which the thickness of each layer is taken as a design variable. This laminate consists of six layers; however, only three of them are treated as design variables due to symmetry. The nondimensional minimum gauge, t_{min}, is set at 0.01, so the design starts from $t_T = 0.03$ where all design variables are at the minimum gauge.

Figure 5 shows the nondimensional height of each layer of the optimum design (above the middle surface) obtained for $0.03 \le t_T \le 0.3$. The thickness of each layer is the distance between the two adjacent heights. In Fig. 5, each curve has three transition points and consists of four solution segments. The circles on the curves indicate the transition points and the dots are the solutions traced along the optimum path. Along the first two segments ($0.03 \le t_T \le 0.185$), the optimum designs are unimodal, and along the last two segments ($0.185 \le t_T \le 0.3$), the optimum designs are bimodal. Along the first segment, only one layer (corresponding to the 45° fibers) varies its thickness, along the second and the third segments two layers (90° and 45°) vary, and along the last

segment all three layers change thickness. In Fig. 6, the nondimensional buckling loads, n_x, corresponding to these optimum designs are shown in semi-log scale for the same range of t_T. The dashed line indicates the buckling loads of reference designs in which all layers have the same thickness. Once all design variables are above their minimum gauges ($t_T \geq 0.274$) we reach the optimum unconstrained ratios of layer thicknesses. These optimum ratios are preserved as we increase the total thickness of the plate, t_T . Above $t_T = 0.274$ the design variables are increased proportionally to t_T, the buckling load is proportional to t_T^3, and the set of active constraints is fixed. Therefore, there is no need to trace the optimal path beyond $t_T = 0.274$.

Next, a $(45°/90°/0°)_s$ laminate is considered. Figure 7 shows the height of each layer of the optimum design for $0.03 \leq t_T \leq 0.05$ and Fig. 8 shows the corresponding nondimensional buckling loads. This path has two transition points and consists of three solution segments. Along the first segment $0.03 \leq t_T \leq 0.0337$ the optimum designs are unimodal, and along the last two segments the optimum designs are bimodal. Along the first segment, only the 0° layer varies its thickness, along the second segment two layers (90° and 0°) vary, and along the last segment ($t_T \geq 0.0449$) all three layers change thickness. The nondimensional buckling load at $t_T > 0.0449$ is obtained by scaling the buckling load at $t_T = 0.0449$ by $(t_T/0.0449)^3$.

It should be noted that the optimum designs at $t_T = 1.0$ give the same buckling loads ($n_x = 16.232$) for both $(0°/90°/45°)_s$ and $(45°/90°/0°)_s$ laminates. The operation described in Section 2 enables us to obtain a $(45°/90°/0°)_s$ design transforming from a $(0°/90°/45°)_s$ design with the same stiffness matrix and the same total thickness. In fact, there are six possible stacking sequences for this case. Designs for all five other sequences were obtained from the $(0°/90°/45°)_s$ design using Eq. (10) and the results are summarized in Table 2. The thickness distribution of the $(45°/90°/0°)_s$ laminate matches the result obtained from the optimization procedure, as it must. The buckling loads for all six designs are the same. Their relationships to the buckling loads for the plate with equal thicknesses are given in the last column of Table 2. In transforming to an equivalent design we assume all the design variables for both designs are free from the bound constraints. Therefore the buckling loads in the two examples are the same when $0.274 \leq t_T \leq 1.0$, where both designs are free from the bound constraints.

In practical design, the thickness of each layer can take only discrete values due to manufacturing requirements. For example, assume that there is a total of 50 plies in the laminate so that each layer is made up from laminas of nondimensional thickness 0.04. The optimal thicknesses from Table 2 are rounded off to the nearest multiple of 0.04. If this leads to a total thickness which is not unity, we modify one of the thickness such that the percentage change from the continuous solution is minimal. The results are presented in Table 3. It is seen that the buckling loads for all six laminates are within 1% of each other and are close to the previous optimal value $n_x = 16.232$.

The existence of equivalent designs with various stacking sequences has two important implications in terms of multiplicity of optimal designs. First, when an optimum design for a given stacking sequence is obtained, all the designs (with the same total thickness and bending stiffnesses) obtained by permuting the stacking sequences are also optimum. This can be proven as follows: If there is another design for a rearranged stacking sequence which has a higher buckling load than the transformed design, a backward transformation should give a design which has a higher buckling load than the optimum design for the original stacking sequence. This is impossible, so the transformed design is also optimum. In fact, the results in Table 2 were verified to be optimum by direct optimization.

Second, for a given stacking sequence, when two or more layers have the same ply orientation, the optimum design is not unique. For example, consider a four-layer $(45°/0°/45°/90°)_s$ laminate with thicknesses t_1, t_2, t_3, and t_4. We can exchange the 0° and 45° layers to get a $(45°/45°/0°/90°)_s$ design with thicknesses t_1, t_2', t_3', t_4, and then change the division between the two adjacent 45° layers. For example, we can redefine the thicknesses as $\frac{1}{2}t_1$, $\frac{1}{2}t_1 + t_2'$, t_3', t_4. Finally, we can switch the adjacent 45° and 0° layers to get a $(45°/0°/45°/90°)_s$ laminate with thicknesses $\frac{1}{2}t_1$, t_2'', t_3'', t_4 , which has the same stacking sequence, the same buckling load and the same total thickness as the original design (so that it is also optimum), but different individual thicknesses.

We reiterate that these properties assume that the thicknesses are not equal to one of their bounds, and that the plate behavior is governed by Eqs. (1), (2), and (11) so the membrane stiffnesses are not included.

Acknowledgment

This work was supported in part by NASA grant NAG-1-168 and AFOSR grant 85-0250.

REFERENCES

1. Chao, C. C., Koh, S. L., and Sun, C. T., "Optimization of Buckling and Yield Strengths of Laminated Composites," AIAA Journal, Vol 13, 1975, 53-66.

2. Chen, T. L. C. and Bert, C. W., "Design of Composite-Material Plates for Maximum Uniaxial Compressive Buckling," Proc. Oklahoma Academy of Science, Vol. 56, 1976, 104-107.

3. Bert, C. W., "Optimal Design of Composite-Material Panels for Business Aircraft," Business Aircraft Meeting of Society of Automotive Engineers, Wichita, Kansas, March 29 - April 1, 1977.

4. Bert, C. W., "Optimal Design of Composite-Material Plate to Maximize its Fundamental Frequency," Journal of Sound and Vibration, Vol. 50, 1977, 229-237.

5. Bert, C. W., "Design of Clamped Composite Plates to Maximize Fundamental Frequency," Journal of Mechanical Design, Vol. 100, 1978, 274-278.

6. Hirano, Y., "Optimum Design of Laminated Plates Under Axial Compression," AIAA Journal, Vol. 17, 1979, 1017-1019.

7. Tauchert, T. R. and Adibhatla, S., "Design of Laminated Plates for Maximum Stiffness," Journal of Composite Materials, Vol. 18, 1984, 58-69.

8. Tauchert, T. R. and Adibhatla, S., "Design of Laminated Plates for Maximum Bending Strength," Engineering Optimization, Vol. 8, 1985, 253-263.

9. Adali, S., "Optimization of Fibre Reinforced Composite Laminates Subject to Fatigue Loading," Proc. of 3rd Int. Conf. on Composite Structures, 9-11 Sept. 1985, Scotland.

10. Pedersen, P., "Minimum Flexibility of Non-Harmonic Loaded Laminated Plates," in Mechanical Characterization of Fibre Composite Materials, ed. R. Pyrz, Aalborg University, Denmark, 1986, 182-196.

11. Lukoshevichyus, R. S., "Minimizing the Mass of Reinforced Rectangular Plates Compressed in Two Directions in a Manner Conducive Toward Stability," Polymer Mechanics, Vol. 12, 1976, 929-933.

12. Schmit, L. A., Jr. and Farshi, B., "Optimum Design of Laminated Fibre Composite Plates," International Journal for Numerical Methods in Engineering, Vol. 11, 1977, 623-640.

13. Starnes, J. H., Jr. and Haftka, R. T., "Preliminary Design of Composite Wings for Buckling, Strength, and Displacement Constraints," Journal of Aircraft, Vol. 16, 1978, 564-570.

14. Rao, S. S. and Singh, K., "Optimum Design of Laminates with Natural Frequency Constraints," Journal of Sound and Vibration, Vol. 67, 1979, 101-112.

15. Anderson, M. S., Stroud, W. J, Durling, B. J., and Hennessy, K. W., "PASCO: Structural Panel Analysis and Sizing Code Users Manual," NASA TM-80182, 1981.

16. Bushnell, D, "PANDA2 - Program for Minimum Weight Design of Stiffened Composite Locally Buckled Panels," Lockheed Palo Alto Research Laboratory, Palo Alto, CA, LMSC-D06775, July, 1986.

17. Mesquita, L. and Kamat, M. P., "Structural Optimization for Control of Stiffened Laminated Composite Using Nonlinear Mixed Integer Programming," Virginia Polytechnic Institute and State University Report, No. VPI-E-85-26, 1985.

18. Mesquita, L. and Kamat, M. P., "Structural Optimization for Control of Stiffened Laminated Composite Structures," Journal of Sound and Vibration, Vol. 116, 1987, 33-48.

19. Olson, G. R. and Vanderplaats, G. N., "A Method for Nonlinear Optimization with Discrete Design Variables," Proceedings of the AIAA/ASME/ASCE/AHS Structures, Structural Dynamics and Materials Conference, Monterey, California, Vol. 1, April, 1987, 343-350.

20. Shin, Y. S., Haftka, R. T., Watson, L. T., and Plaut, R. H., "Tracing Structural Optima as a Function of Available Resources by a Homotopy Method," to be published in Computer Methods in Applied Mechanics and Engineering.

21. Watson, L. T., "Numerical Linear Algebra Aspects of Globally Convergent Homotopy Methods," SIAM Review, Vol. 28, 1986, 529-545.

22. Cohen, G. A., "Effect of Transverse Shear Deformation on Anisotropic Plate Buckling," Journal of Composite Materials, Vol. 16, 1982, 301-312.

23. Bogner, F. K., Fox, R. L., and Schmit, L. A., Jr., "The Generation of Interelement-Compatible Stiffness and Mass Matrices by the Use of Interpolation Formulas," Proc. Conf. Matrix Methods Struct. Mech., Wright-Patterson Air Force Base, Ohio, 1965, AFFDL TR 66-80, 1966.

24. Scott, D. S. and Parlett, B. N., "LASO2," NETLIB, Argonne National Lab., Argonne, IL, 1983.

25. Golub, G. H., Underwood, R., and Wilkinson, J. H., "The Lanczos Algorithm for the Symmetric $Ax = \lambda Bx$ Problem," Report STAN-CS-72-270, Department of Computer Science, Stanford University, Stanford, Calif., 1972.

26. Shin, Y. S., Plaut, R. H., and Haftka, R. T., "Simultaneous Analysis and Design for Eigenvalue Maximization," Proceedings of the AIAA/ASME/ASCE/AHS Structures, Structural Dynamics and Materials Conference, Monterey, California, Vol. 1, April, 1987, 334-342; to be published in AIAA Journal.

APPENDIX Bimodal Formulation

To seek the solutions with double eigenvalues, the problem is formulated assuming bimodality of solutions, or equality of the two lowest eigenvalues, n_{x1} and n_{x2}. The bimodality of the solution results in difficulties in obtaining eigenvalue derivatives. As a remedy, the bimodality constraint is changed slightly so that the two eigenvalues are not exactly the same:

$$n_{x1} - 0.999\, n_{x2} = 0.$$

This equation is included as an additional constraint in forming the augmented function n_x^* :

$$n_x^* = n_{x1} - \gamma[n_{x1} - 0.999\, n_{x2}] - \mu[\sum_{i=1}^{n} t_i - t_T].$$

The stationary conditions are obtained by taking the first derivatives of n_x^* with respect to t_i, γ, and μ and setting them equal to zero. Thus we obtain

i) Optimality conditions

$$(1-\gamma)\frac{\partial n_{x1}}{\partial t_i} + 0.999\,\gamma\frac{\partial n_{x2}}{\partial t_i} - \mu = 0 \qquad \text{for } i \notin I_A$$

ii) Bimodality constraint

$$n_{x1} - 0.999\, n_{x2} = 0$$

iii) Total resource constraint

$$t_T - \sum_{i=1}^{n} t_i = 0.$$

The Lagrange multipliers for the bound constraints, λ_{1i} and λ_{2i} , are required for the transition check. These are obtained by adding the bound constraints to the augmented function n_x* and taking the first derivatives of n_x* with respect to t_i . They are given by

$$\lambda_{1i} = -(1-\gamma)\frac{\partial n_{x1}}{\partial t_i} - 0.999\,\gamma\frac{\partial n_{x2}}{\partial t_i} + \mu \qquad \text{for } t_i = t_{min}$$

$$\lambda_{2i} = (1-\gamma)\frac{\partial n_{x1}}{\partial t_i} + 0.999\,\gamma\frac{\partial n_{x1}}{\partial t_i} - \mu \qquad \text{for } t_i = t_{max}.$$

Table 1. Comparison of buckling loads for different meshes; $(0°/90°/45°)_s$ laminate with $t_1 = t_2 = t_3 = 1/3$

Mesh	2 x 2	3 x 3	4 x 4	5 x 5	6 x 6
First buckling load	11.800	11.742	11.729	11.725	11.724
Second buckling load	27.196	23.369	23.089	23.000	22.969

Table 2. Equivalent optimum designs obtained by permutation of stacking sequence ($t_T = 1.0$)

Stacking sequence of lamina	Reference plate	z_{r+1}	z_r	z_{r-1}	z_*	t_1	t_2	t_3	R[1]
$(0°/90°/45°)_s$	-	-	-	-	-	0.0366	0.1539	0.8095	1.38
$(0°/45°/90°)_s$	$(0°/90°/45°)_s$	0.	0.8095	0.9634	0.7139	0.0366	0.2496	0.7139	1.31
$(45°/0°/90°)_s$	$(0°/45°/90°)_s$	0.7139	0.9634	1.0	0.7772	0.2228	0.0634	0.7139	1.12
$(45°/90°/0°)_s$	$(45°/0°/90°)_s$	0.	0.7139	0.7772	0.4729	0.2228	0.3044	0.4729	1.03
$(90°/45°/0°)_s$	$(45°/90°/0°)_s$	0.4729	0.7772	1.0	0.8601	0.1399	0.3872	0.4729	1.32
$(90°/0°/45°)_s$	$(90°/45°/0°)_s$	0.	0.4729	0.8601	0.8095	0.1399	0.0506	0.8095	1.17

[1] R is the ratio of the optimal buckling load to the buckling load when $t_1 = t_2 = t_3 = 1/3$.

Table 3. Buckling loads for 6 optimal laminates with integer number of plies

Stacking sequence of lamina	t_1	t_2	t_3	n_x
$(0°/90°_4/45°_{20})_s$	0.04	0.16	0.80	16.21
$(0°/45°_6/90°_{18})_s$	0.04	0.24	0.72	16.21
$(45°_5/0°_2/90°_{18})_s$	0.20	0.08	0.72	16.09
$(45°_5/90°_8/0°_{12})_s$	0.20	0.32	0.48	16.05
$(90°_3/45°_{10}/0°_{12})_s$	0.12	0.40	0.48	16.10
$(90°_3/0°/45°_{21})_s$	0.12	0.04	0.84	16.19

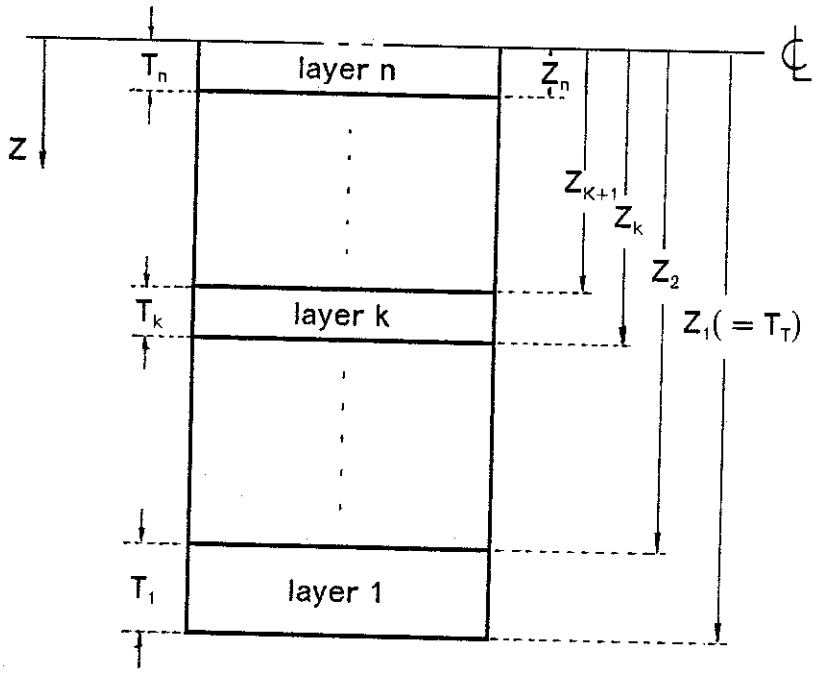

Figure 1: Geometry of half of a 2n-layered symmetric laminate

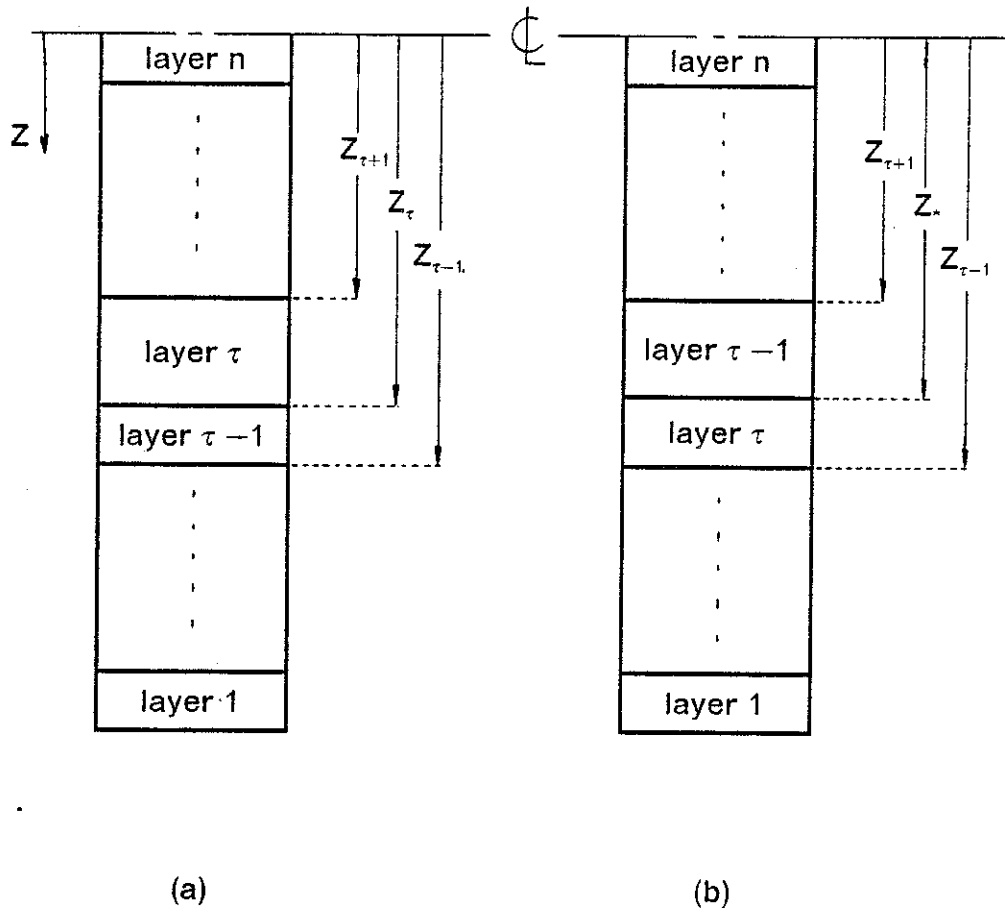

Figure 2: Symmetric 2n-layered laminates

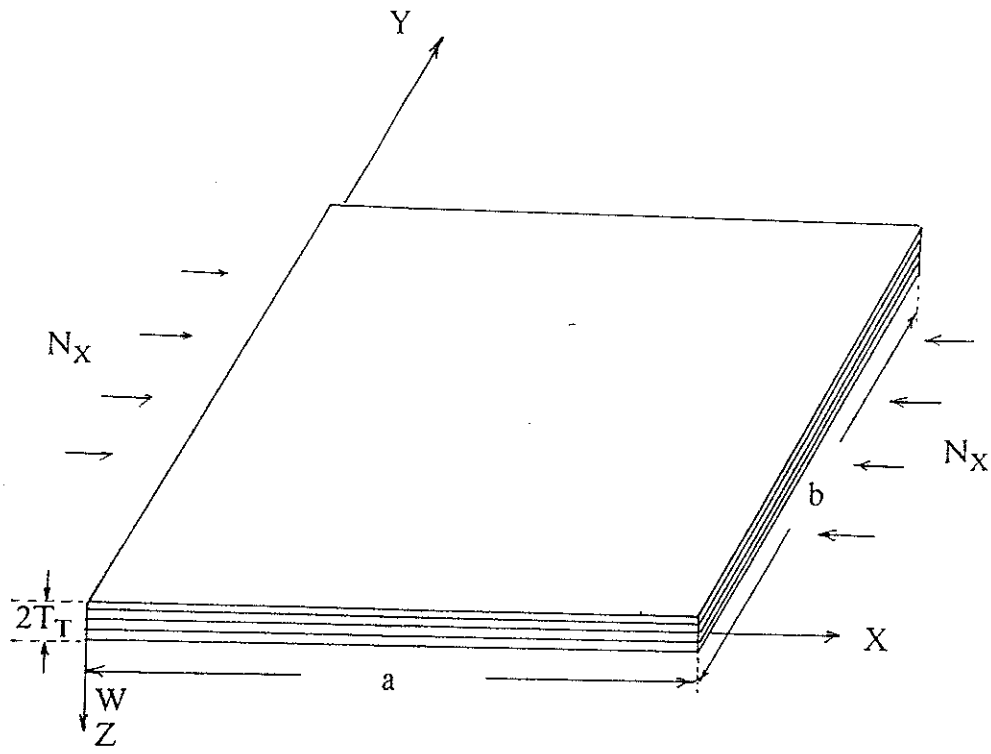

Figure 3: Geometry of plate under uniform uniaxial in-plane load

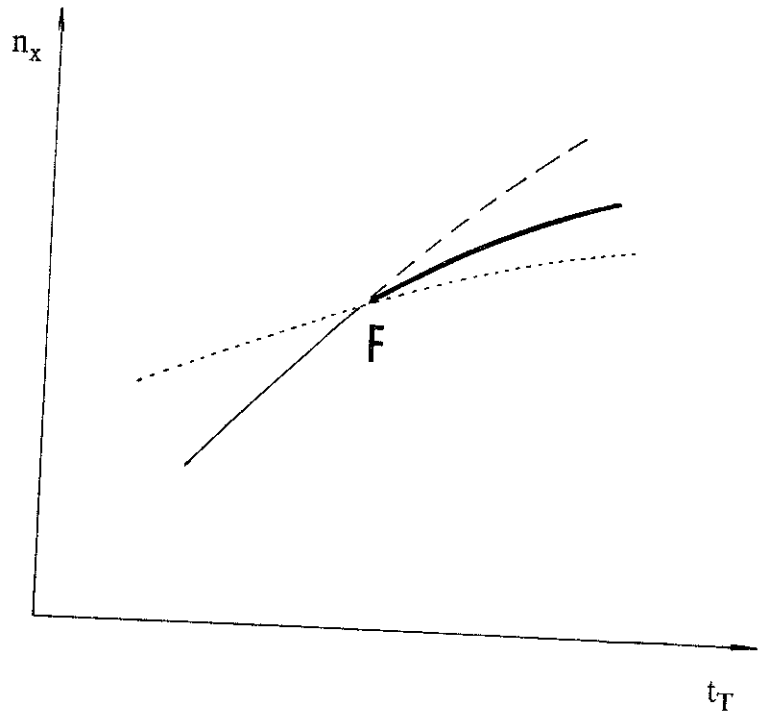

F : Transition point

——— : Path corresponding to mode 1 (Optimum unimodal path)

..... : Path corresponding to mode 2

– – – – : Artificial path for mode 1

▬▬ : Optimum bimodal path

Figure 4: Transition from unimodal to bimodal segment

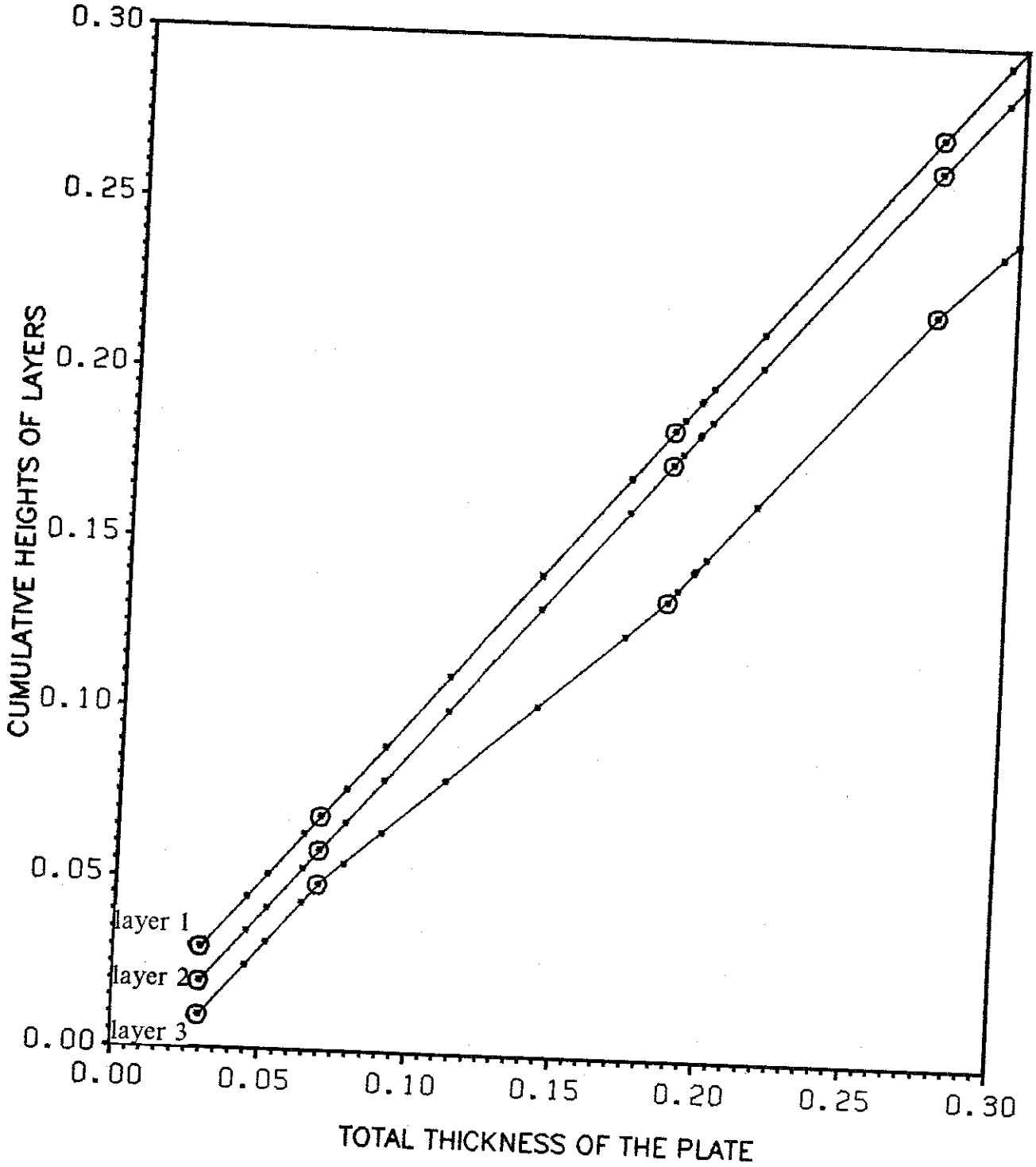

Figure 5: Optimum thickness distributions for (0°/90°/45°), laminates

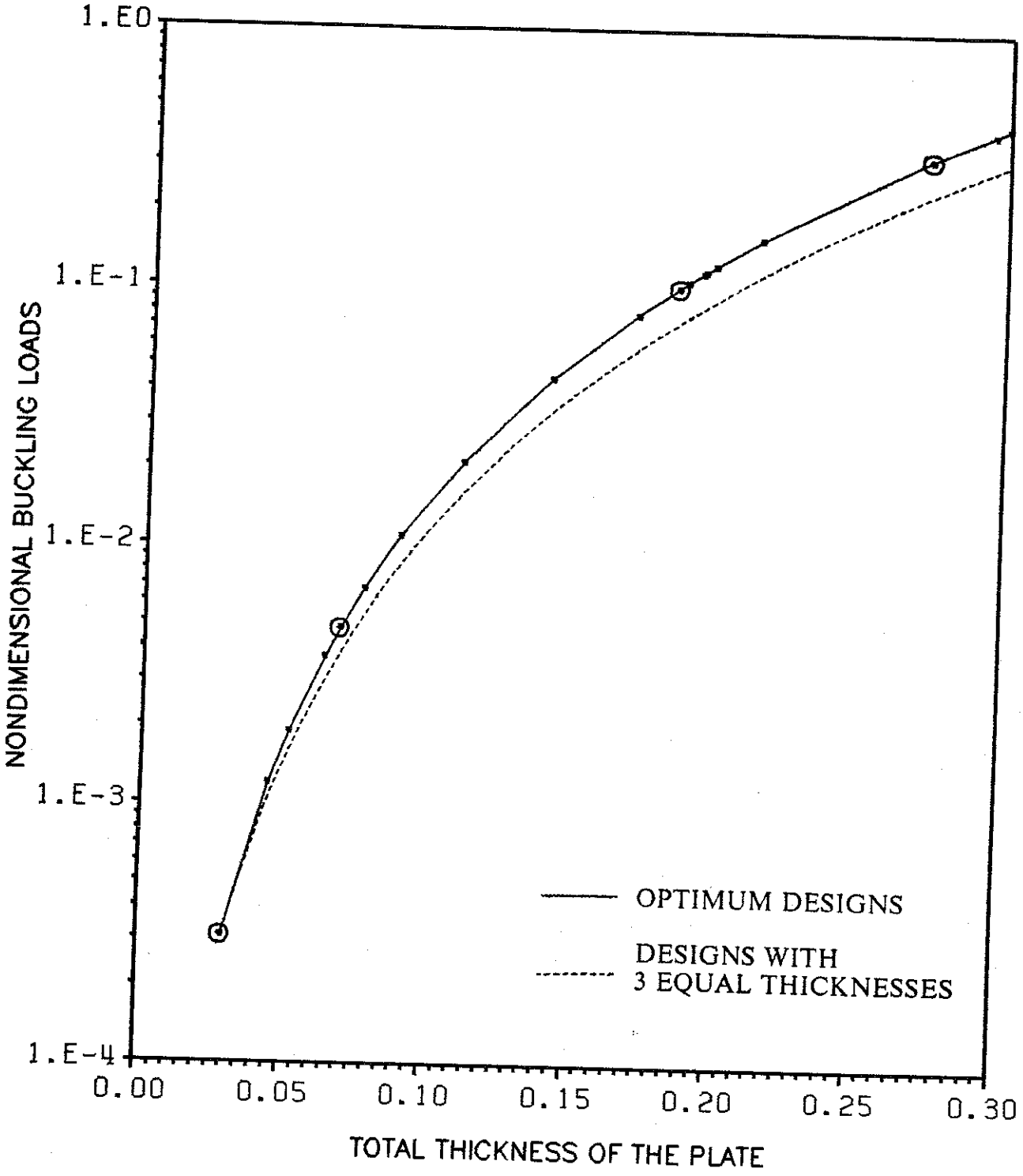

Figure 6: Buckling loads for optimum and equal thickness (0°/90°/45°) laminates

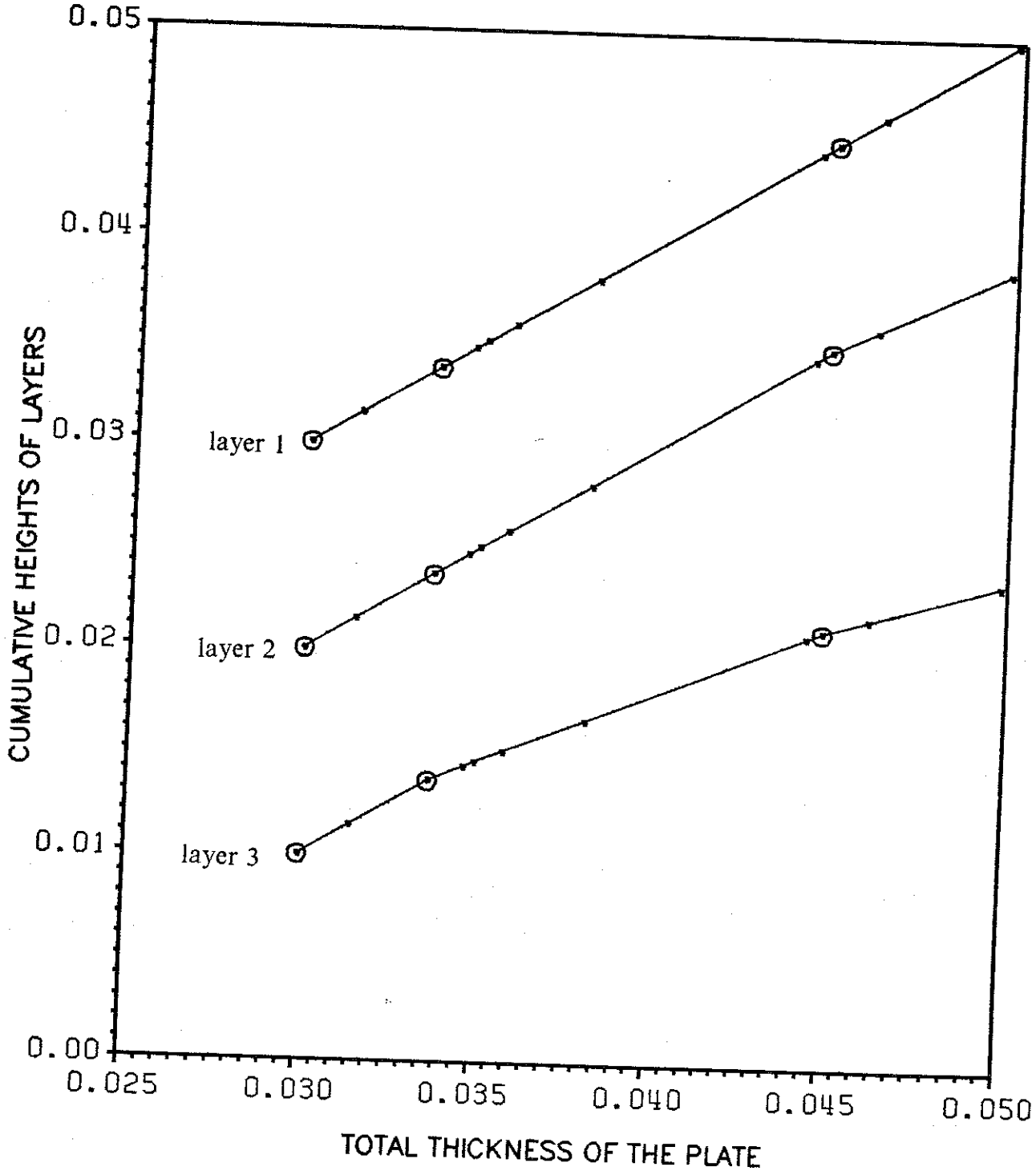

Figure 7: Optimum thickness distributions for (45°/90°/0°), laminates

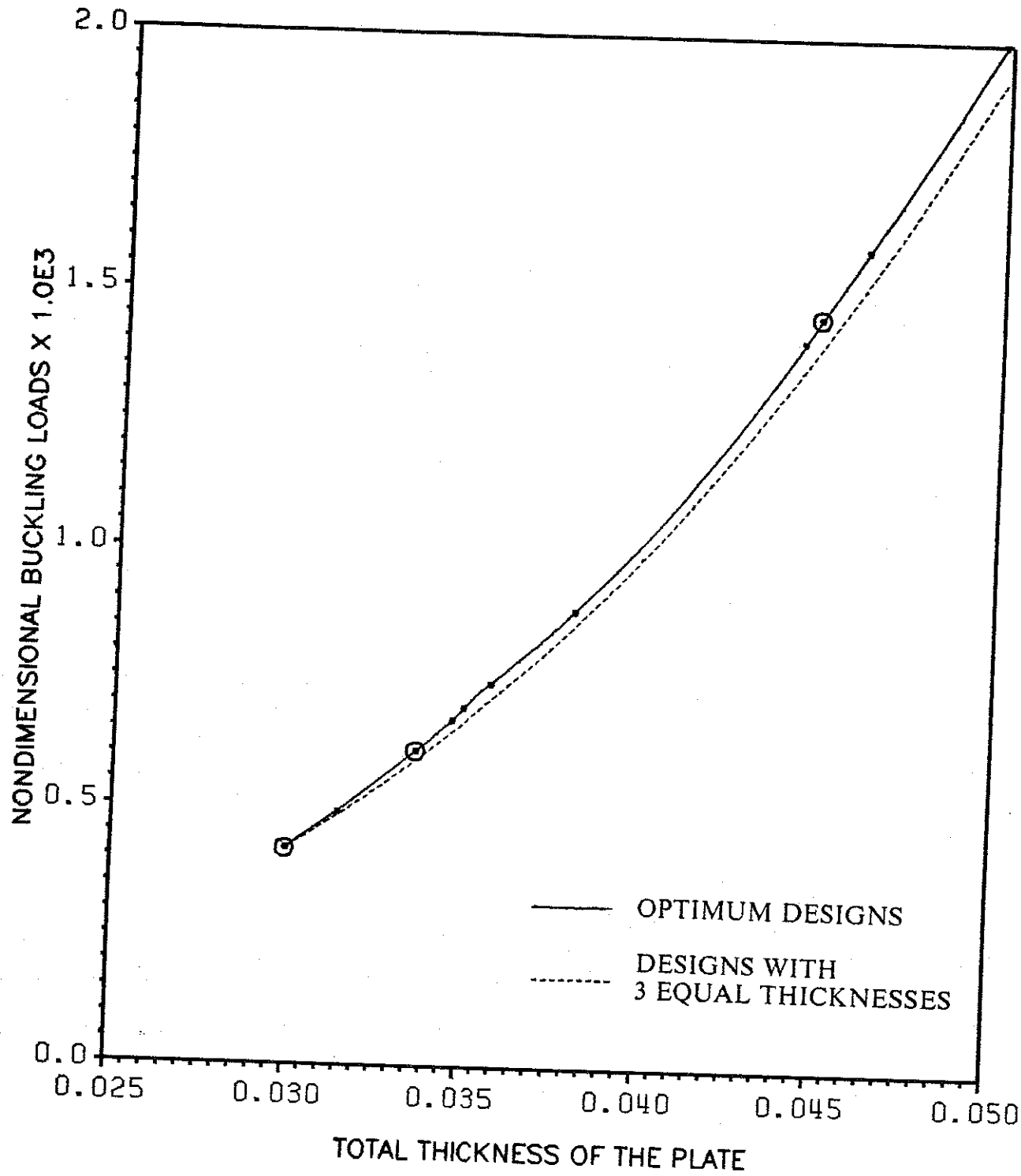

Figure 8: Buckling loads for optimum and equal thickness (45°/90°/0°) laminates